RHEUMATOLOGY

Rheumatology 2021;00:1–11
https://doi.org/10.1093/rheumatology/keab904
Advance access publication 9 December 2021

Original article

Parvovirus B19 induces cellular senescence in human dermal fibroblasts: putative role in systemic sclerosis–associated fibrosis

Rosaria Arvia[1], Krystyna Zakrzewska[1], Lisa Giovannelli[2], Sara Ristori[2], Elena Frediani[3], Mario Del Rosso[3], Alessandra Mocali[3], Maria A Stincarelli[1], Anna Laurenzana[3], Gabriella Fibbi[3] and Francesca Margheri [3]

Abstract

Objective. Emerging evidence demonstrates that excessive accumulation of senescent cells is associated with some chronic diseases and suggests a pathogenic role of cellular senescence in fibrotic processes, such as that occurring in ageing or in SSc. Recently we demonstrated that parvovirus B19 (B19V) activates normal human dermal fibroblasts and induces expression of different profibrotic/pro-inflammatory genes. This observation prompted us to investigate whether it is also able to induce fibroblast senescence as a potential pathogenetic mechanism in B19V-induced fibrosis.

Methods. Primary cultures of fibroblasts were infected with B19V and analysed for the acquisition of senescence markers, such as morphological modifications, senescence-associated β-galactosidase (SA-β-gal) activity, DNA damage response and expression of senescence-associated secretory phenotype (SASP)-related factors.

Results. We demonstrated that B19V-infected fibroblasts develop typical senescence features such as enlarged and flat-shaped morphology and SA-β-gal activity similar to that observed in SSc skin fibroblasts. They also developed an SASP-like phenotype characterized by mRNA expression and release of some pro-inflammatory cytokines, along with activation of the transcription factor nuclear factor κB. Moreover, we observed B19V-induced DNA damage with the comet assay: a subpopulation of fibroblasts from B19V-infected cultures showed a significantly higher level of DNA strand breaks and oxidative damage compared with mock-infected cells. An increased level and nuclear localization of γH2AX, a hallmark of DNA damage response, were also found.

Conclusions. B19V-induced senescence and production of SASP-like factors in normal dermal fibroblasts could represent a new pathogenic mechanism of non-productive B19V infection, which may have a role in the fibrotic process.

Key words: parvovirus B19, cellular senescence, SSc, fibrosis, normal human dermal fibroblasts

Rheumatology key messages

- B19V infection in dermal fibroblasts leads to cellular senescence and release of SASP factors.
- B19V-infected fibroblast cultures show a significantly higher level of DNA strand breaks and oxidative damage.
- B19V-induced senescence could play a role in SSc-associated fibrosis.

Introduction

Cellular senescence is a state of permanent cell cycle arrest in which senescent cells do not replicate but remain viable and metabolically active. The most characteristic hallmarks of senescent cells are persistent DNA damage response (DDR) activation; permanent cell cycle arrest; morphological changes characterized by an enlarged flattened shape, vacuolization and multinucleation; increased

[1]Department of Experimental and Clinical Medicine, [2]Department NEUROFARBA, Section of Pharmacology and Toxicology and [3]Department of Experimental and Clinical Biomedical Sciences 'Mario Serio', University of Florence, Florence, Italy

Submitted 21 July 2021; accepted 29 November 2021

Correspondence to: Krystyna Zakrzewska, Department of Experimental and Clinical Medicine, University of Florence, viale Morgagni 48, 50134, Florence, Italy.
E-mail: krystyna.zakrzewska@unifi.it

BASIC SCIENCE

levels of senescence-associated β-galactosidase (SA-β-gal) activity; upregulation of antiproliferative factors and acquisition of the senescence-associated secretory phenotype (SASP), characterized by release of a variety of cytokines, growth factors, proteases and chemokines [1].

Emerging evidence demonstrates that excessive accumulation of senescent cells is associated with some chronic diseases and suggests a pathogenic role of cellular senescence in the fibrotic process, such as that occurring in ageing or in SSc [2].

SSc, a connective tissue disease that leads to fibrosis in multiple organs, including skin, heart, vasculature and lungs, is not typically considered a disease of ageing. Nevertheless, SSc-associated fibrosis shares some pathological features (epithelial and endothelial injury, immune dysregulation and fibroblasts activation with increased deposition of extracellular matrix) with other age-related fibrotic diseases, such as idiopathic pulmonary fibrosis [3]. Furthermore, several studies have shown that advanced age is associated with a higher incidence and more severe course of disease and with increased mortality of SSc patients [4, 5], suggesting the association of SSc with ageing.

Moreover, Ogawa *et al.* [6] demonstrated that SA-β-gal expression was higher in SSc skin than in healthy controls. The SA-β-gal expression was observed in sclerotic skin lesions of SSc patients, while it was not detected in non-sclerotic lesions of SSc patients. Furthermore, cultured fibroblasts from SSc patients showed higher SA-β-gal expression than control fibroblasts [6]. These data suggest that cellular senescence in SSc fibroblasts may contribute to disease development.

The study of Dumit *et al.* [7], employing a proteomic approach, identified numerous age-dependent differences, including the accumulation of SA-β-gal, and showed that SSc fibroblasts displayed evidence indicative of cellular senescence.

The pathogenesis of SSc is multifactorial, and the exact mechanisms involved in the activation of fibroblasts leading to severe cutaneous and systemic fibrosis are not fully understood [8, 9]. A role of different environmental factors has been hypothesized, including toxic and microbial agents that could trigger the fibrotic process in genetically predisposed subjects. Some viral infections seem to play a role in the onset and/or progression of SSc. One of the viruses likely involved is parvovirus B19 (B19V) [10–13].

B19V is a small, non-enveloped ssDNA virus with an icosahedral capsid composed of two structural proteins, VP1 and VP2. The major non-structural protein, NS1, is involved in viral replication and in the pathogenesis of some B19V-associated diseases [14]. B19V infection is associated with a wide range of clinical manifestations [15]. After primary infection, B19V DNA persists lifelong in several tissues, mainly in bone marrow, heart, liver synovia and skin [16]. The functional consequences of such persistence are still unknown.

Cellular senescence can be induced by different stimuli, including virus infection and virus-induced stress response pathways, such as oxidative stress or DDR and IFN signalling. In fact, it has been demonstrated that persistent treatment with IFN-β induces a DNA damage signalling pathway and senescence [17].

The induction of senescence in response to virus infection can result from the activation of different pathways. The activation of DDR and induction of senescence was demonstrated for human respiratory syncytial virus [18] and for dengue virus [19] and the senescence process has been proposed to contribute to the pathologic features induced by these viruses. HCV and HBV can also induce senescence. Senescent hepatocytes were found in chronic HCV infection and a correlation between liver fibrosis, chronic HCV infections and cellular senescence has been reported [20]. Analysis of liver tissue from patients with chronic HBV infection also revealed an association between fibrosis, HBV infection and senescence-associated markers [21]. Finally, one of the few pathologies clearly associated with both senescence and virus infection is HIV-related osteoporosis and OA [22].

In the course of natural infection, B19V targets erythroid progenitor cells (EPCs), which are permissive for viral replication [23]. It has been demonstrated that in CD36 EPC cultures, B19V NS1 protein induces stable cell cycle arrest, which increases viral replication [24]. Moreover, B19V DNA replication induces DDR, with activation of all three phosphatidylinositol 3-kinase–related kinases (PI3KKs): DNA-dependent protein kinase catalytic subunit (DNA-PKcs), ataxia telangiectasia mutated (ATM) protein kinase activated by double-stranded breaks and ataxia telangiectasia and Rad3-related (ATR) activated by single-stranded breaks [25].

It is known that B19V can also infect different types of non-erythroid cells in a non-productive manner, characterized by the presence of viral DNA and/or limited expression of viral mRNAs and proteins [26, 27]. It has been demonstrated that such an abortive infection can activate different cellular pathways associated with morphological and functional cellular modifications and cytokine production [26].

Recently we demonstrated that primary human dermal fibroblasts incubated with B19V showed a significant increase of both migration and invasiveness, along with mRNA expression of different profibrotic genes, with some genes associated with the inflammasome platform and genes for metalloproteases, suggesting that the virus might have a role in the pathogenesis of fibrosis [27]. This observation, indicating that B19V can activate dermal fibroblasts and induce production of SASP-like factors, prompted us to investigate whether it is also able to induce fibroblast senescence as a potential pathogenetic mechanism in B19V-induced fibrosis.

In the present study, primary cultures of skin fibroblasts were infected with B19V and, at different time points post-infection, were analysed for the acquisition of senescence markers, such as morphological features, SA-β-gal activity, DNA damage markers and expression of some SASP-related factors by means of mRNA and protein production and release.

Materials and methods

Cell cultures

Normal human dermal fibroblasts (NHDFs) obtained from a pool of adult donors (Sigma-Aldrich, St. Louis, MO, USA; 106-05A) were cultured in DMEM with 10% foetal bovine serum (FBS). SSc fibroblasts at early cell culture passages (2–3; SSc1 and SSc2) already present in our cell repository were used in this study as senescence controls. SSc had been previously isolated from affected dorsal skin of the hands, as previously described [28], after approval of the local ethics committee of Azienda Ospedaliero–Universitaria Careggi di Firenze. All patients provided written informed consent (see Supplementary Data S1, available at *Rheumatology* online, for details).

Cell cycle synchronization

NHDFs were seeded in a six-well plate at a density of 1.2×10^5 cells/well in DMEM with FBS at 10%. For synchronization of the G0/G1 phase, a serum-deprivation method was used to treat NHDFs. See details in Supplementary Data S1, available at *Rheumatology* online.

Assessment of cell cycle with flow cytometric analysis

After 72 h in DMEM with 0.2% FBS and 96 h in DMEM with FBS 10%, the assessment of cell cycle in fibroblast cells was performed using propidium iodide solution (Sigma-Aldrich). See details in Supplementary Data S1, available at *Rheumatology* online.

B19V infection of NHDFs

After synchronization and the percentage of cells in S-phase was determined, NHDFs were counted and infected as previously described [27]. See details in Supplementary Data S1, available at *Rheumatology* online.

Nucleic acids extraction and amplification to detect B19V infection markers

Real-time PCR to quantify B19V DNA and B19V NS1 mRNA and qualitative PCR to detect spliced B19V transcripts were carried out as previously described [27]. See details in Supplementary Data S1, available at *Rheumatology* online.

Expression studies

At 3 days post-infection, NHDFs were analysed to study mRNA expression of selected genes, such as IL-1α, IL-1β, IL-6 and IL-8, as previously described [27]. See details in Supplementary Data S1, available at *Rheumatology* online.

SA-β-gal assay

For the assessment of SA-β-gal activity, cells were seeded at a density of 10–20 cells/cm^2. SA-β-gal staining was performed according to Dimri *et al.* [29]. See details in Supplementary Data S1, available at *Rheumatology* online.

Immunofluorescence for B19V-VP proteins and SA-β-gal

At 4 days post-infection, NHDFs were harvested and seeded onto glass slides at a density of 1×10^5 and allowed to adhere. Cells were washed twice in PBS and allowed to dry. Glass slides were fixed for 10 min in 2% paraformaldehyde, incubated overnight with Cell Event Senescence Green Probe (C10850; Invitrogen, Carlsbad, CA, USA) and labelled with anti-VP1/VP2 monoclonal antibody as previously described [27]. See details in Supplementary Data S1, available at *Rheumatology* online.

Immunofluorescence for γH2AX and nuclear factor κB [NF-κB (p65)]

Confocal immunofluorescence analysis for NF-κB (p65) was performed as previously described [30]. γH2AX immunofluorescence was performed according to the same protocol for NF-κB. See details in Supplementary Data S1, available at *Rheumatology* online.

Measurement of DNA strand breaks and oxidized bases with the comet assay

Aliquots of the cells (60 000 cells in 60 μL) were resuspended in freezing medium (culture medium containing 40% FBS and 10% DMSO) and stored at −80°C. The frozen samples were defrosted and analysed for DNA damage by a comet assay, as previously described [31]. See details in Supplementary Data S1, available at *Rheumatology* online.

Preparation of conditioned media

For conditioned media preparation, DMEM plus 2% FBS was added, after washing with PBS, to NHDF cell cultures in a ratio of 1 ml/150 000 cells. Conditioned media were collected after 6 and 24 h incubation from mock-infected fibroblasts and B19V-infected fibroblasts at 3 and 7 days post-infection and centrifuged at 1500 rpm for 5 min. All media were stored at −80°C until use.

ELISA for cytokines detection

IL-6, IL-1β and IL-8 were detected in cell-conditioned media with Mini TMB ELISA Development Kits (PeproTech, Cranbury, NJ, USA) according to the manufacturer's instructions, as previously described [32, 33].

Statistical analysis

For the expression studies, statistical analysis was performed using the Student's two-tailed *t*-test. *P*-values <0.05 were considered significant.

Results

B19V infection in NHDFs leads to cellular senescence

The growing cell culture contains cells in all phases of their reproductive cycle, and in each phase the cells could exhibit different susceptibility to B19V infection and to expression of the senescence markers, introducing high variability of results obtained in different settings. To overcome this problem, in all experiments, synchronized cell cultures via the serum deprivation method were infected. To confirm the cell synchronization, after 72 h in DMEM with 0.2% FBS and 96 h in DMEM with FBS 10%, we examined the cell cycle by FACS analysis. We observed that the synchronized cultures contained ~80% of cells in the S-phase (Supplementary Fig. S1, available at *Rheumatology* online).

In line with our previous studies [27, 34], in infected cultures we detected viral DNA, B19V NS1 transcripts and spliced viral mRNAs during the entire time course of infection (from day 3 through day 12 post-infection) without significant quantitative changes over that time (Fig. 1A and B). Moreover, at 4 days post-infection, ~26% of infected cells were positive for the VP1/VP2 proteins by immunofluorescence analysis (Fig. 1C).

To determine whether B19V infection induced cellular senescence, we analysed in B19V-infected fibroblasts the acquisition of senescence markers, such as morphological features and SA-β-gal activity. In order to establish a direct correlation between the viral infection and the cellular senescence, we performed a confocal immunofluorescence analysis for the B19V VP1 and VP2 proteins and for SA-β-gal activity using the Cell Event Senescence Green probe, a fluorescent reagent specific to β-galactosidase. Fig. 1C shows an evident co-localization of VP1/VP2 with the SA-β-gal green probe in B19V-infected fibroblasts compared with mock-infected cells. As reported in the histogram (Fig. 1C, on the right), the percentage of SA-β-gal and VP1/VP2-positive cells was significantly higher in B19V-infected cells compared with mock-infected NHDFs. These data demonstrated that B19V-infected NHDFs are also positive to SA-β-gal staining. To evaluate over time the acquisition of SA-β-gal activity in infected cells, we performed the SA-β-gal colorimetric staining at 3, 7 and 12 days post-infection. Compared with mock-infected cells, B19V-infected NHDFs showed a significant increase, with approximately a doubled percentage, of SA-β-gal-positive cells at any time of observation (203%, 205%, 180% and 164%, respectively) (Fig. 2A), suggesting that the B19V-infected cells acquired SA-β-gal activity, similar to that observed in SSc fibroblasts (SSc1 and SSc2) (Fig. 2B) and previously reported [6]. In addition, compared with mock-infected fibroblasts, B19V-infected cells, as well as SSc fibroblasts, exhibited characteristic features of senescent cells, such as a flattened and enlarged morphology.

B19V causes DNA damage in NHDFs

The persistent activation of a DDR is important for the establishment and maintenance of cellular senescence [35, 36]. To examine the DNA damage in B19V-infected cells, we performed a confocal immunofluorescence analysis of γH2AX at 3, 7, and 12 days post-infection. Fig. 3 shows that the number of γH2AX foci-containing cells was significantly higher in B19V-infected fibroblasts compared with mock-infected cells at 3 and 12 days of observations (438% at 3 days and 361% at 12 days). In parallel, we used the single-cell gel electrophoresis method (comet assay) to measure both single-strand breaks and oxidized bases [measured as formamidopyrimidine DNA glycosylase (FPG)-sensitive sites]. The analysis of the mean values indicated an increase in both types of DNA damage, mainly at 3 days, which was not statistically significant (data not shown). Instead, the frequency distribution analysis for DNA strand breaks revealed an increased number of highly damaged cells in the B19V group compared with mock-infected cells (from 3.5 to 10% of the total at 3 days; Fig. 4A and B). Using a cut-off at 15% tail DNA, we were able to show a statistically significant increase in damaged cells in the B19V group at 3 and 12 days (Fig. 4C). The same analysis carried out on total DNA damage (to which the main contribution was from oxidative damage) showed a strong reduction in non-damaged cells at 3 days in the B19V group (from 29% in mock-infected cells to 3.5% in B19V) (Fig. 4D and E), and the cut-off analysis (set at 22% tail DNA) confirmed a statistically significant effect at 3 and not at 7 or 12 days (Fig. 4F).

B19V induces NF-κB activation and SASP-related cytokine release

In addition to phenotypical and molecular features, senescent cells are characterized by the up-regulation and release of several pro-inflammatory cytokines, growth factors and proteases, the so-called SASP. As DNA damage promotes the SASP program in senescent cells, through NF-κB activation, we examined in B19V-infected NHDFs the NF-κB nuclear localization by immunofluorescence. Fig. 5 (A and B) shows that B19V infection induced at 4 days post-infection an increment in NF-κB nuclear localization, measured by Mander's coefficient M1 (175% increase; $P < 0.0293$). Consequently, we analysed the mRNA expression level of IL-1α , IL-1β, IL-6 and IL-8, the well-known SASP cytokines. Compared with mock-infected cells, the B19V-infected fibroblasts showed a significant increase in mRNA expression of IL-1α (fold change 4.2; $P = 0.014$), IL-1β (fold change 3.6; $P = 0.0007$), IL-6 (fold change 3.3; $P = 0.01$) and IL-8 (fold change 2.2; $P = 0.00000$) at 3 days post-infection (Fig. 5C). In parallel, we measured the level of IL-1β, IL-6 and IL-8 released in mock-infected and B19V-NHDF conditioned media, collected after 6 h from the addition of DMEM

FIG. 1 Time course of B19V infection of primary NHDF cultures

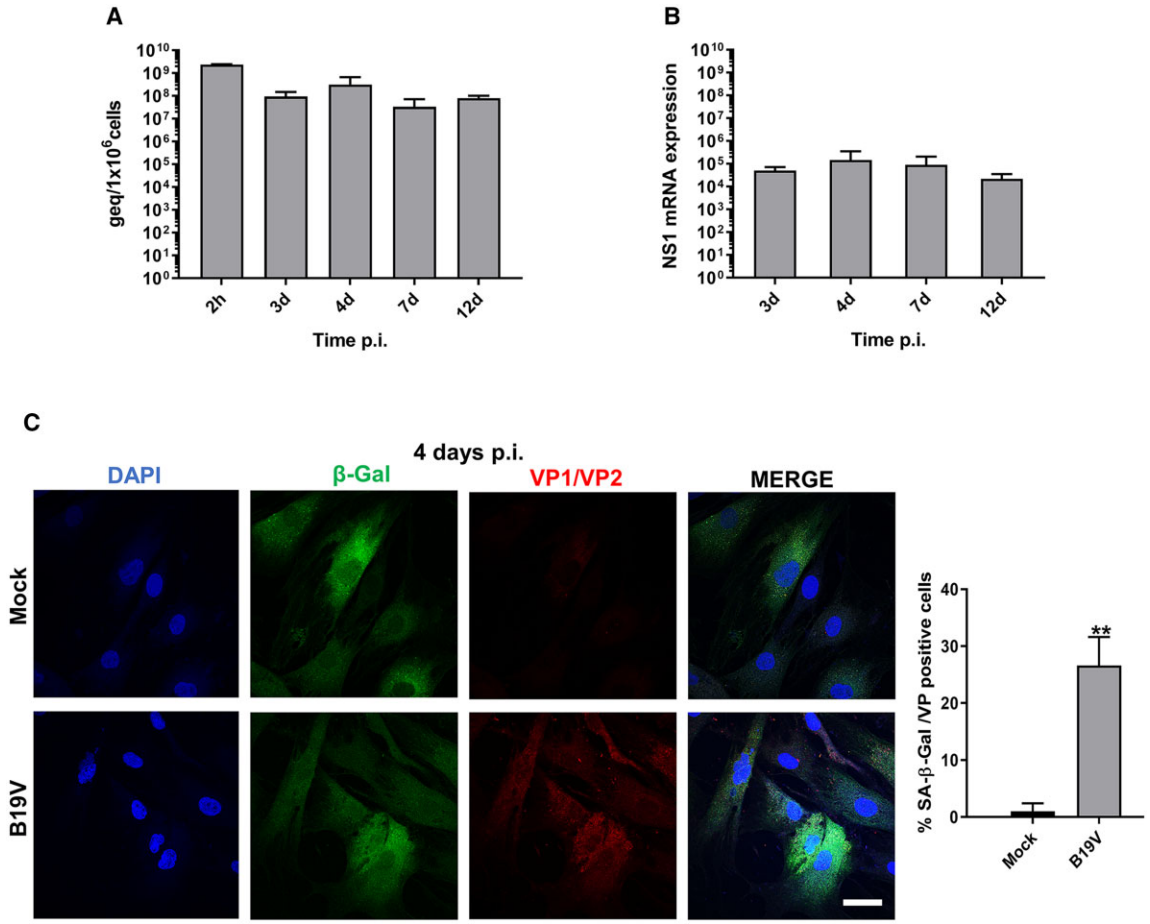

(**A**) The levels of viral DNA were evaluated at the end of the absorption/penetration period 2 h post-infection and at 3, 4, 7 and 12 days post-infection. (**B**) The mRNAs for NS1 protein were carried out at 3, 4, 7 and 12 days post-infection. Bars are the mean (S.E.) of four independent cultures. (**C**) Confocal immunofluorescence assay for the detection of B19V VP1/VP2 proteins and SA-β-gal activity with the β-gal green fluorescent probe at 4 days post-infection. Histogram, on the left, shows the percentage of VP1/VP2 and SA-β-gal-positive cells in B19-infected cells compared with mock-infected fibroblasts. Bars represent the mean (S.E.) values of five different photographic fields. Scale bar = 50 μm. *$P < 0.05$ *vs* mock-infected cells.

2% FBS, at 3 and 7 days post-infection. As shown in Fig. 5D, a consistent increased release of all tested cytokines in extracellular media was observed in B19V-NHDFs compared with mock-infected cells.

Discussion

B19V has been proposed as a cofactor in the pathogenesis of some autoimmune diseases [14]. The involvement of B19V infection in SSc is supported by some epidemiological and experimental studies that demonstrated, compared with healthy subjects, SSc patients showed a higher prevalence of B19V DNA in the bone marrow, the main target of the virus, and in the skin, as well as higher prevalence of anti-B19V NS1 antibodies, a marker of persistent infection [10]. Further, fibroblasts, endothelia and perivascular inflammatory cells of the skin from SSc patients showed the presence of both B19V and mRNA expression and TNF-α mRNAs [12].

In the course of natural infection, B19V targets erythroid progenitor cells in the bone marrow, which are permissive for viral replication. Moreover, B19V can also infect different types of non-erythroid cells in a non-productive manner, characterized by the presence of viral DNA and/or limited expression of viral mRNAs and proteins. It has been demonstrated that such an abortive infection can activate different cellular pathways associated with morphological and functional cellular modifications and cytokine production [26]. In fact, in a previous study we demonstrated that B19V abortive infection increases TNF-α production and induces NLRP3-mediated caspase-1 activation and IL-1β secretion in monocytic PMA-differentiated THP-1 cells and that

FIG. 2 B19V infection in NHDFs leads to cellular senescence

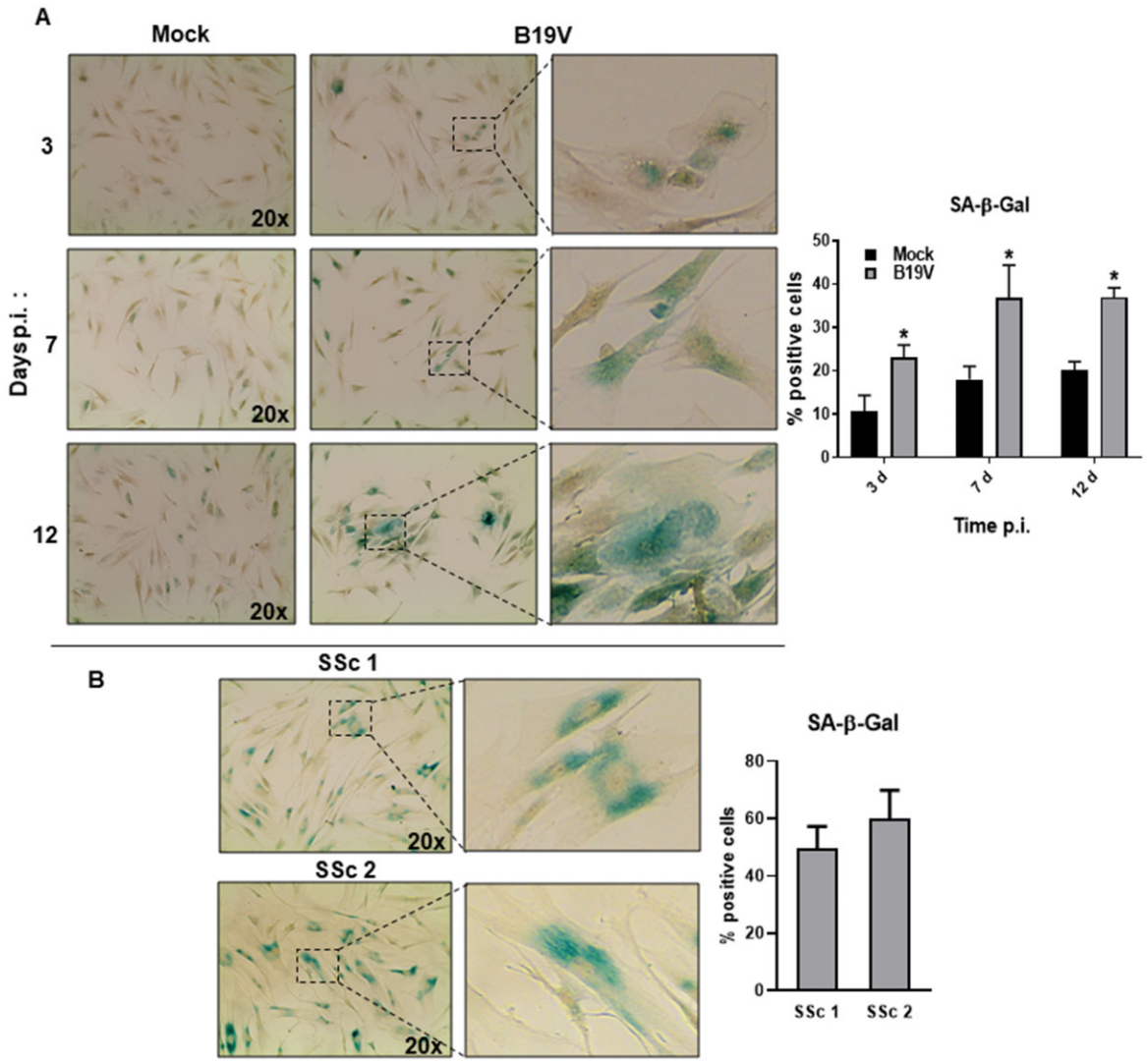

(**A**) Percentage of SA-β-gal-positive cells at 3, 7 and 12 days post-infection and (**B**) in SSc uninfected fibroblasts by colorimetric β-gal activity assay. Representative images of SA-β-gal-positive cells are reported (on the left, $\times$200 magnification). Bars are the mean (S.E.) of three experiments. *$P < 0.05$ *vs* mock-infected cells.

B19V-infected monocytes from scleroderma patients express NLRP3 and activate caspase-1 [13].

In vitro studies provided evidence that B19V can infect the target cells of SSc, such as dermal fibroblasts and endothelial cells [27, 34], and can persist in SSc skin fibroblasts propagated *in vitro* [11]. *In vitro*, infected fibroblast B19V DNA, viral transcripts and structural proteins were detected [27]. However, the pathogenetic consequences of infection in fibroblasts is still unknown. Emerging evidence suggests a pathogenetic role of cellular senescence in the fibrotic process, such as that occurring in ageing or in systemic sclerosis [2].

In our previous study we demonstrated that B19V is able to activate dermal fibroblasts and induce expression of a pool of SASP-like factors [27]. In fact, we observed that primary human dermal fibroblasts incubated with B19V showed a significant increase of both migration and invasiveness, along with mRNA expression of different profibrotic genes, some genes associated with the inflammasome platform and genes for metalloprotease, suggesting that the virus might play a role in the pathogenesis of fibrosis.

As these features are also typical of senescent fibroblasts [37], in the present work we aimed to investigate whether B19V is able to induce fibroblast senescence. Indeed, the present data indicate that senescence induction is involved in the functional alterations induced by B19V infection in dermal fibroblasts.

In the present study we showed that B19V-infected dermal fibroblasts acquire a series of senescence

FIG. 3 B19V infection induces γH2AX activation in NHDFs

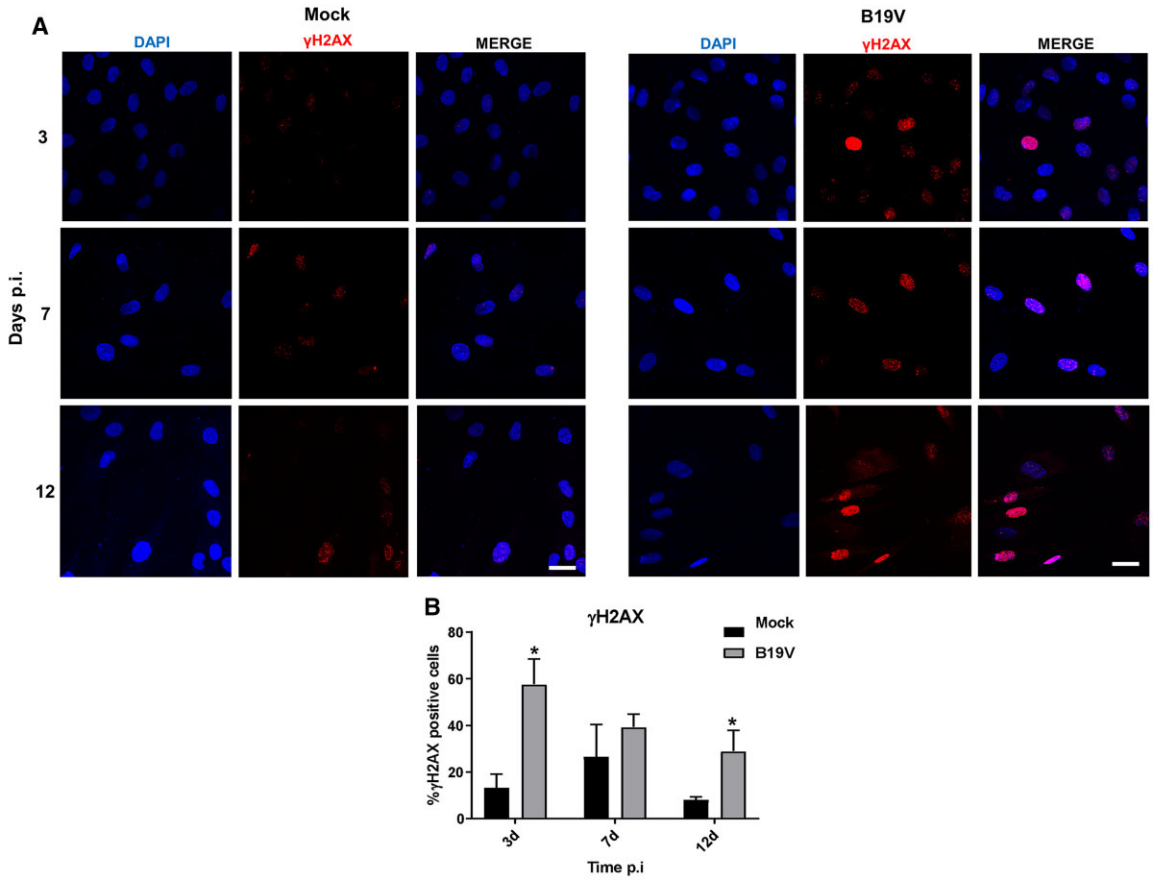

(**A**) Confocal immunofluorescence assay for the detection of γH2AX foci in B19V-infected NHDFs compared with mock-infected fibroblasts at 3, 7 and 12 days post-infection. Scale bar = 50 μm. (**B**) Histogram reports the percentage of γH2AX-positive cells in B19V-infected fibroblasts compared with mock-infected cells at 3, 7 and 12 days post-infection. Bars are the mean (S.E.) of five different photographic fields. *$P < 0.05$ *vs* mock-infected cells.

markers, including typical enlarged and flat-shaped morphology and SA-β-gal activity. In particular, we observed a co-localization between SA-β-gal green fluorescent probe and VP1/VP2 viral proteins, demonstrating that B19V-infected NHDFs are also positive to SA-β-Gal staining. Taken together, these data indicate that viral infection induces senescence in dermal fibroblasts.

Moreover, in agreement with our previous results [27], B19V-infected NHDFs developed a SASP-like phenotype characterized by mRNA expression for some pro-inflammatory cytokines, such as IL-1α, IL-1β, IL-6 and IL-8, and by release of IL-1β, IL-6 and IL-8, due to the activation of transcription factor NF-κB. The SASP is a hallmark of senescent cells and can affect the cellular environment and homeostasis of the neighbouring tissues [38, 39]. Although the SASP phenotype could restrict damage propagation and activate immune responses, two essential processes involved in response to viral infections, the excessive accumulation and persistence of senescent cells can become detrimental, promoting pathology and dysfunctions [40]. In our context, we showed that B19V-infected fibroblasts, through the SASP-associated phenotype, could induce paracrine senescence in neighbouring cells, contributing to propagation of senescence. Indeed, we found that the percentage of SA-β-gal-positive cells was greater than that of B19V-infected fibroblasts, suggesting that the B19V infection can trigger and transmit cellular senescence to neighbouring cells. Long *et al.* [41] demonstrated that latent EBV infection in EBV-positive cells triggers the SASP in neighbouring epithelial cells and, in contrast, lytic EBV infection abolishes this phenotype.

In order to replicate, viruses must interact with their hosts and these interactions often provoke the DDR that represents an important inductor of senescence. The DDR can be activated by incoming viral DNA, during the integration of some viruses such as retroviruses or adeno-associated viruses or as a response to the aberrant DNA structures generated upon replication of DNA viruses. Furthermore, DDR can be induced by viral proteins that can stimulate inappropriate S-phase entry, modify cellular DDR factors directly or bind and damage host DNA [42].

A large variety of viruses could damage cellular DNA. For example, adenovirus 12 induces chromosomal

FIG. 4 B19V infection induces DNA damage in NHDFs

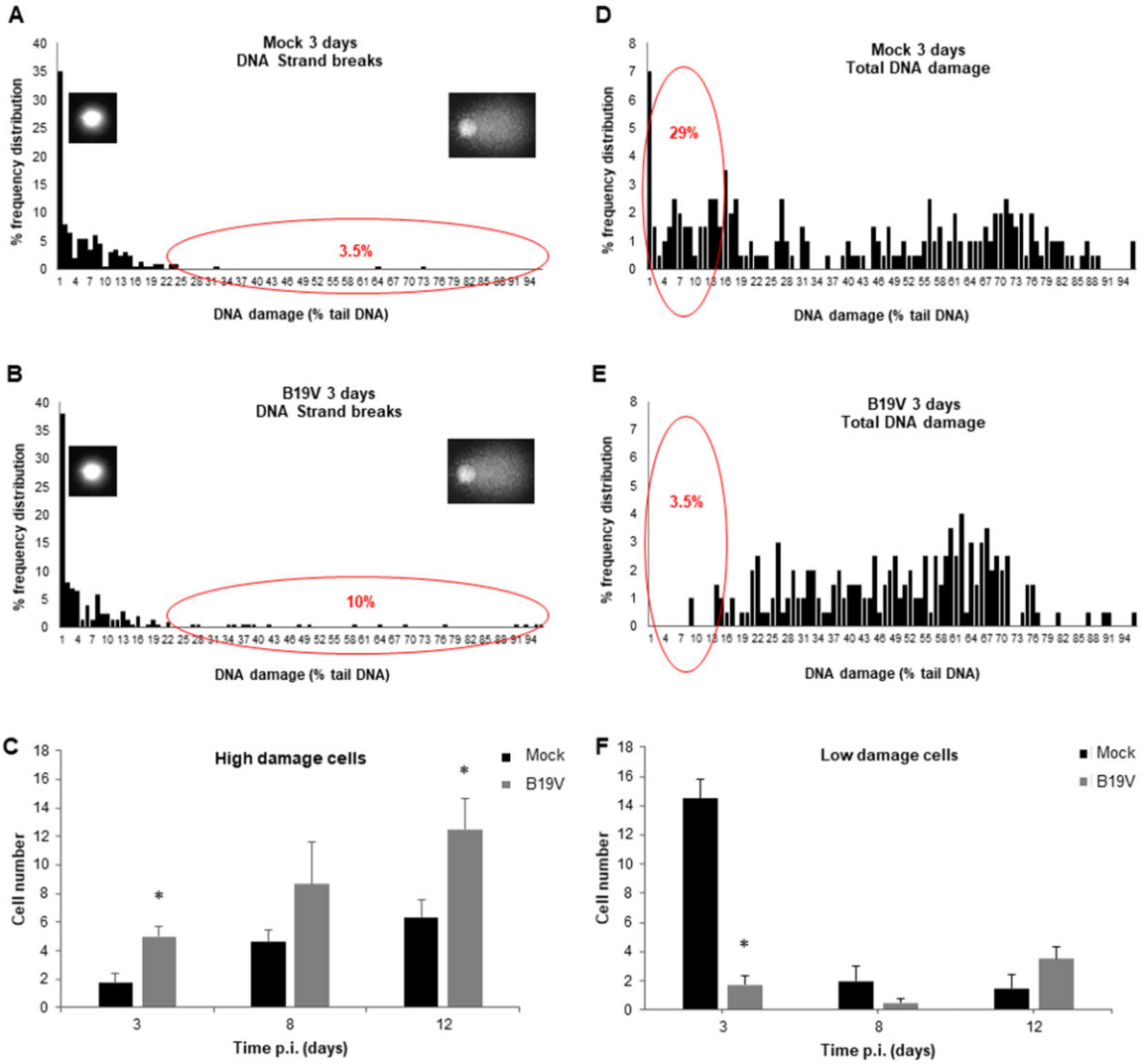

Frequency distribution of DNA strand breaks in the analysed cell sample for (**A**) mock- and (**B**) B19V-infected cells. DNA damage on the *x*-axis is expressed as the percentage of tail DNA and two examples of comet images depict no damage on the left and high damage on the right of the axis. The classes of cells with DNA damage >15% tail DNA are highlighted by a red ellipse and the corresponding total percentage over the total is shown in red. (**C**) Number of cells with DNA strand breaks >15% tail DNA in mock- and B19V-infected cells at the three investigated times post-infection. Numbers are the average cell count in each duplicate [mean (S.E.) of three experiments]. *$P < 0.05$ *vs* mock-infected cells. Frequency distribution of DNA total damage (strand breaks + FPG sites) in the analysed cell sample for (**D**) mock- and (**E**) B19V-infected cells. The classes of cells with DNA damage <22% tail DNA are highlighted by a red ellipse and the corresponding total percentage over the total is shown in red. (**F**) Number of cells with DNA total damage <22% tail DNA in mock- and B19V-infected cells at the three investigated times post-infection. Numbers are the average cell count in each duplicate [mean (S.E.) of three experiments]. *$P < 0.05$ *vs* mock-infected cells.

aberration in HEK293 cells [43]. Chromosomal lesions have been observed in cells infected with simian virus 40, HSV, human cytomegalovirus and EBV [44].

As an ssDNA virus, B19V induces a broad range of DDRs by targeting activation of all PI3KKs associated with the DNA repair pathway during productive infection in EPCs and both the ATR and DNA-PK are essential to promote replication of its genome. It has been demonstrated that viral DNA replication, but not viral proteins, is required for B19V-induced DDR. Moreover, expression of NS1 protein, a multifunctional protein with NTP binding, helicase, endonuclease and transactivation activities [45], is sufficient to induce G2/M arrest and apoptosis [46] in EPC. On the other hand, in non-permissive cell line HepG2, DDR induction has been associated with the activity of B19V NS1 protein, being

FIG. 5 B19V induces NF-κB activation and SASP-related cytokine release

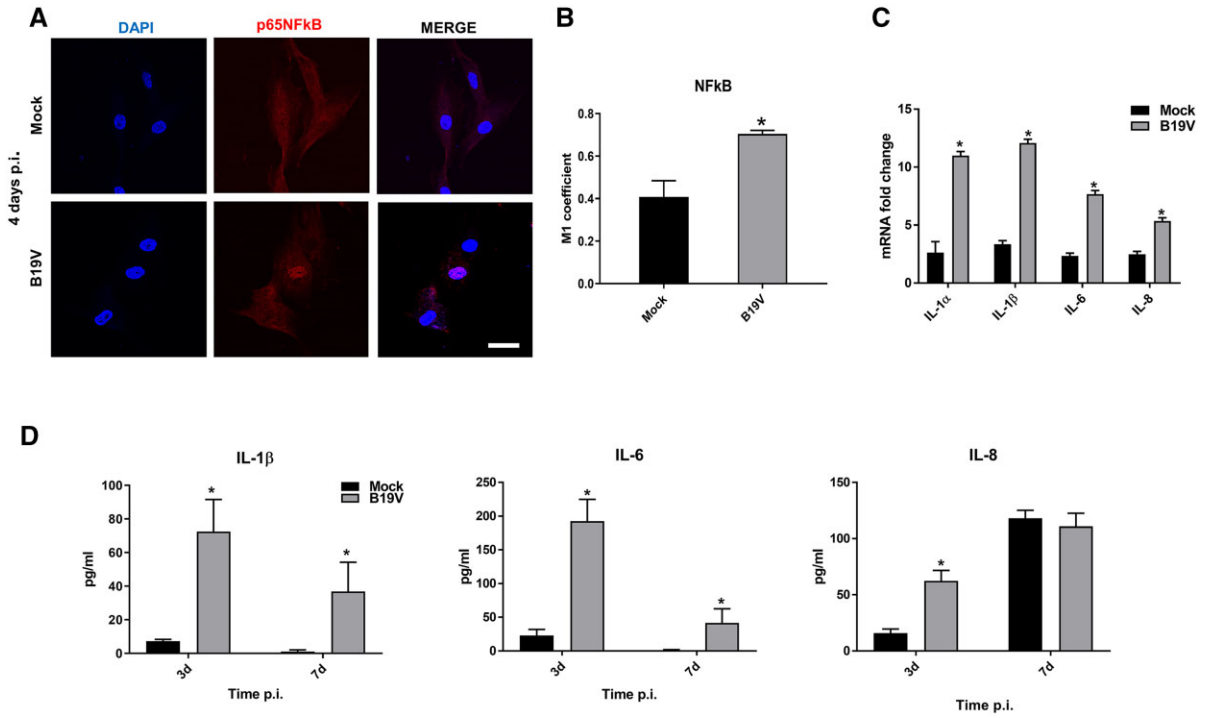

(**A**) NF-κB intracellular localization analysed by confocal immunofluorescence. Scale bar = 100 μm. (**B**) Histogram shows NF-κB fluorescence nuclear localization (NF-κB/DAPI) by Mander's coefficient (M1) using ImageJ software. Bars are the mean (S.E.) of three experiments. *$P < 0.05$ *vs* mock-infected cells. (**C**) mRNA expression of IL-1α, IL-1β, IL-6 and IL-8 in B19V-infected and mock cultures at 3 days post-infection. Data are expressed as the fold change normalized to mRNA of the housekeeping gene. Bars represent mean (S.E.M.) of three different experiments. *P*-values were calculated using a two-tailed *t*-test. *$P < 0.05$. (**D**) IL-1β, IL-6 and IL-8 quantification in conditioned media collected from B19V- and mock-infected NHDFs by ELISA at 3 and 7 days post-infection 6 h after the DMEM 2% FBS addition. Histograms report pg/ml of the selected cytokines. Bars are the mean (S.E.) of three experiments. *$P < 0.05$ *vs* mock-infected cells.

able to nick cellular chromosomes and cause damage to host DNA, leading to apoptosis [47].

In the present study we observed B19V-induced DNA damage analysed with the comet assay. Namely, a subpopulation of fibroblasts from B19V-infected cultures showed a significantly higher level of DNA strand breaks and oxidative damage compared with mock-infected cells. An increased level and nuclear localization of γH2AX, a hallmark of DDR, were also found.

Generally, DDR can lead to three distinct outcomes. In the context of mild damage, it may recruit the repair machinery and induce cell cycle arrest [48]. When DNA injury is severe and irreversible, the host cell may undergo senescence or cell death programs. Whether the damaged cell undergoes apoptosis or senescence depends on the cell type, physiological context and nature and intensity of the damage [49] and may have different pathological consequences.

B19V-induced apoptosis of EPCs leads to aplastic crisis (in the acute phase) or to pure cell aplasia (in the chronic phase), especially in subjects with shortened red cell survival or in immunocompromised patients. B19V-infected hepatocytes undergo apoptosis, which has been proposed as the mechanism of B19V-associated acute fulminant liver failure [50].

B19V-induced senescence and production of SASP-like factors in normal dermal fibroblasts could represent a new pathogenic mechanism, not described previously, of viral infection in these cells. Further studies will be required to determine the possible mechanisms involved in B19V-induced senescence in NHDFs and the role of the virus in the fibrotic process.

Acknowledgments

The authors thank Kedrion (Barga, Italy) for the generous gift of B19V viraemic plasma. This work was supported by a grant from the Ministero dell'Istruzione, dell'Università e della Ricerca 'Progetti di Rilevante Interesse Nazionale 2015' (grant 2015YZB22C-002 LS6; CUP: B16J15001970001) and by Foundation 'Istituto di Ricerca Virologica Oretta Bartolomei Corsi', Florence, Italy and partially supported by the Ministry of Education, Universities and Research of Italy [Progetto Dipartimenti

di Eccellenza 'Gender Medicine' (to C.D.)]. The data presented in the current study were generated in part using the equipment of the Facility of Molecular Medicine, funded by the Ministry of Education, Universities and Research of Italy, Dipartimenti di Eccellenza 2018–2022.

Funding: This work was supported by a grant from Ministero dell'Istruzione, dell'Università e della Ricerca 'Progetti di Rilevante Interesse Nazionale 2015' (grant 2015YZB22C-002 LS6; CUP: B16J15001970001) and by the Foundation 'Istituto di Ricerca Virologica Oretta Bartolomei Corsi', Florence, Italy and by Ente Cassa di Risparmio, Florence, Italy. The funders had no role in the data collection and analysis, decision to publish or preparation of the manuscript.

Disclosure statement: The authors have declared no conflicts of interest.

Data availability statement

The data underlying this article will be shared on request to the corresponding author.

Supplementary data

Supplementary data are available at *Rheumatology* online.

References

1 Gorgoulis V, Adams PD, Alimonti A *et al.* Cellular senescence: defining a path forward. Cell 2019;179:813–27.

2 Schafer MJ, Haak AJ, Tschumperlin DJ, LeBrasseur NK. Targeting senescent cells in fibrosis: pathology, paradox, and practical considerations. Curr Rheumatol Rep 2018;20:3.

3 Herzog EL, Mathur A, Tager AM *et al.* Review: interstitial lung disease associated with systemic sclerosis and idiopathic pulmonary fibrosis: how similar and distinct? Arthritis Rheumatol 2014;66:1967–78.

4 Manno RL, Wigley FM, Gelber AC, Hummers LK. Late-age onset systemic sclerosis. J Rheumatol 2011;38:1317–25.

5 Strickland G, Pauling J, Cavill C, Shaddick G, McHugh N. Mortality in systemic sclerosis-a single center study from the UK. Clin Rheumatol 2013;32:1533–9.

6 Ogawa F, Tomita H, Koike Y *et al.* AB0229 Senescence associated β-galactosisdase expression in systemic sclerosis skin and fibroblasts. Ann Rheum Dis 2013;71:650.

7 Dumit VI, Küttner V, Käppler J *et al.* Altered MCM protein levels and autophagic flux in aged and systemic sclerosis dermal fibroblasts. J Invest Dermatol 2014;134:2321–30.

8 Bhattacharyya S, Wei J, Varga J. Understanding fibrosis in systemic sclerosis: shifting paradigms, emerging opportunities. Nat Rev Rheumatol 2011;25:42–54.

9 Katsumoto TR, Whitfield ML, Connolly MK. The pathogenesis of systemic sclerosis. Ann Rev Pathol 2011;6:509–37.

10 Ferri C, Zakrzewska K, Longombardo G *et al.* Parvovirus B19 infection of bone marrow in systemic sclerosis patients. Clin Exp Rheumatol 1999;17:718–20.

11 Ferri C, Giuggioli D, Sebastiani M *et al.* Parvovirus B19 infection of cultured skin fibroblasts from systemic sclerosis patients: comment on the article by Ray et al. Arthritis Rheum 2002;46:2262–3; author reply 2263–4.

12 Magro CM, Nuovo G, Ferri C *et al.* Parvoviral infection of endothelial cells and stromal fibroblasts: a possible pathogenetic role in scleroderma. J Cutan Pathol 2004;31:43–50.

13 Zakrzewska K, Arvia R, Torcia MG *et al.* Effects of parvovirus B19 in vitro infection on monocytes from patients with systemic sclerosis: enhanced inflammatory pathways by caspase-1 activation and cytokine production. J Invest Dermatol 2019;139:2125–33.

14 Kerr JR. The role of parvovirus B19 in the pathogenesis of autoimmunity and autoimmune disease. J Clin Pathol 2016;69:279–91.

15 Young NS, Brown KE. Parvovirus B19. N Engl J Med 2004;350:586–97.

16 Norja P, Hokynar K, Aaltonen LM *et al.* Bioportfolio: lifelong persistence of variant and prototypic erythrovirus DNA genomes in human tissue. Proc Natl Acad Sci USA 2006;103:7450–3.

17 Moiseeva O, Mallette FA, Mukhopadhyay UK, Moores A, Ferbeyre G. DNA damage signaling and p53-dependent senescence after prolonged beta-interferon stimulation. Mol Biol Cell 2006;17:1583–92.

18 Martínez I, García-Carpizo V, Guijarro T *et al.* Induction of DNA double-strand breaks and cellular senescence by human respiratory syncytial virus. Virulence 2016;7:427–442.

19 AbuBakar S, Shu MH, Johari J, Wong PF. Senescence affects endothelial cells susceptibility to dengue virus infection. Int J Med Sci 2014;11:538–44.

20 Paradis V, Youssef N, Dargère D *et al.* Replicative senescence in normal liver, chronic hepatitis C, and hepatocellular carcinomas. Hum Pathol 2001;32:327–32.

21 Tachtatzis PM, Marshall A, Arvinthan A *et al.* Chronic hepatitis B virus infection: the relation between hepatitis B antigen expression, telomere length, senescence, inflammation and fibrosis. PLoS One 2015;10:e0127511.

22 Beaupere C, Garcia M, Larghero J *et al.* The HIV proteins Tat and Nef promote human bone marrow mesenchymal stem cell senescence and alter osteoblastic differentiation. Aging Cell 2015;14:534–46.

23 Ozawa K, Kurtzman G, Young N. Productive infection by B19 parvovirus of human erythroid bone marrow cells in vitro. Blood 1987;70:384–91.

24 Morita E, Nakashima A, Asao H, Sato H, Sugamura K. Human parvovirus B19 nonstructural protein (NS1) induces cell cycle arrest at G(1) phase. J Virol 2003;77:2915–21.

25 Luo Y, Lou S, Deng X *et al.* Parvovirus B19 infection of human primary erythroid progenitor cells triggers ATR-

Chk1 signaling, which promotes B19 virus replication. J Virol 2011;85:8046–55.

26 Adamson-Small LA, Ignatovich IV, Laemmerhirt MG, Hobbs JA. Persistent parvovirus B19 infection in non-erythroid tissues: possible role in the inflammatory and disease process. Virus Res 2014;190:8–16.

27 Arvia R, Margheri F, Stincarelli MA *et al.* Parvovirus B19 activates in vitro normal human dermal fibroblasts: a possible implication in skin fibrosis and systemic sclerosis. Rheumatology 2020;59:3526–32.

28 Serratì S, Cinelli M, Margheri F *et al.* Systemic sclerosis fibroblasts inhibit in vitro angiogenesis by MMP-12-dependent cleavage of the endothelial cell urokinase receptor. J Pathol 2006;210:240–8.

29 Dimri M, Carroll JD, Cho JH, Dimri GP. microRNA-141 regulates BMI1 expression and induces senescence in human diploid fibroblasts. Cell Cycle 2013;12:3537–46.

30 Menicacci B, Cipriani C, Margheri F, Mocali A, Giovannelli L. Modulation of the senescence-associated inflammatory phenotype in human fibroblasts by olive phenols. Int J Mol Sci 2017;18:2275.

31 Ladeira C, Koppen G, Scavone F, Giovannelli L. The comet assay for human biomonitoring: effect of cryopreservation on DNA damage in different blood cell preparations. Mutat Res 2019;843:11–7.

32 Menicacci B, Margheri F, Laurenzana A *et al.* Chronic resveratrol treatment reduces the pro-angiogenic effect of human fibroblast "senescent-associated secretory phenotype" on endothelial colony-forming cells: the role of IL8. J Gerontol A Biol Sci Med Sci 2019;74:625–33.

33 Margheri F, Menicacci B, Laurenzana A *et al.* Oleuropein aglycone attenuates the pro-angiogenic phenotype of senescent fibroblasts: a functional study in endothelial cells. J Funct Foods 2019;53:219–26.

34 Zakrzewska K, Cortivo R, Tonello C *et al.* Human parvovirus B19 experimental infection in human fibroblasts and endothelial cells cultures. Virus Res 2005;114:1–5.

35 Bartkova J, Rezaei N, Liontos M *et al.* Oncogene-induced senescence is part of the tumorigenesis barrier imposed by DNA damage checkpoints. Nature 2006;444:633–7.

36 Di Micco R, Fumagalli M, Cicalese A *et al.* Oncogene-induced senescence is a DNA damage response triggered by DNA hyper-replication. Nature 2006;444:638–42.

37 Lin Y, Xu Z. Fibroblast senescence in idiopathic pulmonary fibrosis. Front Cell Dev Biol 2020;8:593283.

38 Acosta JC, Banito A, Wuestefeld T *et al.* A complex secretory program orchestrated by the inflammasome controls paracrine senescence. Nat Cell Biol 2013;15:978–90.

39 Coppé JP, Desprez PY, Krtolica A, Campisi J. The senescence-associated secretory phenotype: the dark side of tumor suppression. Annu Rev Pathol 2010;5:99–118.

40 Kohli J, Veenstra I, Demaria M. The struggle of a good friend getting old: cellular senescence in viral responses and therapy. EMBO Rep 2021;22:e52243.

41 Long X, Li Y, Yang M *et al.* BZLF1 attenuates transmission of inflammatory paracrine senescence in Epstein-Barr virus-infected cells by downregulating tumor necrosis factor alpha. J Virol 2016;90:7880–93.

42 Lufting MA. Viruses and the DNA damage response: activation and antagonism. Annu Rev Virol 2014;1:605–25.

43 Zur Hausen H. Induction of specific chromosomal aberrations by adenovirus type 12 in human embryonic kidney cells. J Virol 1967;1:1174–85.

44 Fortunato EA, Spector DH. Viral induction of site-specific chromosome damage. Rev Med Virol 2003;13:21–37.

45 Fu Y, Ishii KK, Munakata Y *et al.* Regulation of tumor necrosis factor alpha promoter by human parvovirus B19 NS1 through activation of AP-1 and AP-2. J Virol 2002;76:5395–403.

46 Moffatt S, Yaegashi N, Tada K, Tanaka N, Sugamura K. Human parvovirus B19 nonstructural (NS1) protein induces apoptosis in erythroid lineage cells. J Virol 1998;72:3018–28.

47 Poole BD, Kivovich V, Gilbert L, Naides SJ. Parvovirus B19 nonstructural protein-induced damage of cellular DNA and resultant apoptosis. Int J Med Sci 2011;8:88–96.

48 Ljungman M. The DNA damage response—repair or despair? Environ Mol Mutagen 2010;51:879–89.

49 Surova O, Zhivotovsky B. Various modes of cell death induced by DNA damage. Oncogene 2013;32:3789–97.

50 Poole BD, Karetnyi YV, Naides SJ. Parvovirus B19-induced apoptosis of hepatocytes. J Virol 2004;78:7775–83.